



ISSN: 2785-2997

Journal of Human, Earth, and Future

Vol. 2, No. 4, December, 2021



Investigation Optical Properties of the Orthorhombic System $CsSnBr_{3-x}I_x$: Application for Solar Cells and Optoelectronic Devices

Nematov Dilshod Davlatshoevich ^{1, 2*}

¹ *S.U. Umarov Physical-Technical Institute of the National Academy of Science of Tajikistan, Dushanbe, Tajikistan*

² *Osimi Tajik Technical University, 724000, Dushanbe, Tajikistan*

Received 24 September 2021; Revised 23 November 2021; Accepted 27 November 2021; Published 01 December 2021

Abstract

In this work, to study the optical properties of orthorhombic perovskites of the $CsSnBr_{3-x}I_x$ system, spin-orbital and spin-polarized quantum chemical calculations were carried out in the framework of the density functional theory. The effects of electron exchange correlation were taken into account by the modified Becke-Jones exchange-correlation potential (*mBJ*). It has been established that with an increase in the iodine concentration, the absorption capacity and photoconductivity of these semiconductors increase. Other optical properties were also calculated, such as the real and imaginary parts of the dielectric function, refractive indices, energy loss spectrum, extinction coefficients, and reflection coefficients. The high absorption of these compounds in the infrared, visible and ultraviolet energy ranges allows the use of these perovskites in optical and optoelectronic devices operating in all spectral ranges by controlling and changing their content.

Keywords: Density Functional Theory; Optical Band Gap; Perovskite; Optical Absorption; Photoconductivity; Dielectric Constant; Energy; Reflectivity.

1. Introduction

The family of perovskite nanocrystals with the general formula ABX_3 (where A is a positive ion, B is a metal ion, and X is a halogen anion) is of considerable interest to the scientific community and is a promising class of materials due to many interesting physical and chemical properties such as high thermal and photoelectric power, superconductivity, ferroelectricity, spin-dependent transport, charge ordering, colossal magnetoresistance and other excellent structural, magnetic and optical properties [1-3]. These materials are often used as sensors, substrates, catalytic electrodes in fuel cells, photonic devices such as lasers, LEDs, and especially solar cells due to their high absorption of visible light with a narrow bandgap, excellent charge carrier mobility, high dielectric constant, high conductivity, reduced reflectivity, reduced charge carrier recombination rate, and low excitation energy binding. They are promising candidates for optoelectronics [4].

A new application of perovskites has been found in a hybrid organo-inorganic material that has been used in thin film solar cells and transistors [5]. On the other hand, metal halide semiconductor materials are currently more efficient and beneficial for use in photovoltaic applications compared to silicon-based technologies. It is reported that the conversion efficiency of a perovskite solar cell already reaches 26% [6]. In addition, perovskite materials are available at low cost, and therefore, research on these materials has shown rapid progress in the scientific community

* Corresponding author: dilnem@mail.ru

<http://dx.doi.org/10.28991/HEF-2021-02-04-08>

➤ This is an open access article under the CC-BY license (<https://creativecommons.org/licenses/by/4.0/>).

© Authors retain all copyrights.

as well as their potential use in photovoltaic applications. Due to their excellent energy conversion efficiency in photovoltaic devices, halide perovskites have generated considerable interest among other perovskite compounds. Compounds based on the $CsSnBr_{3-x}I_x$ system have interesting optical and electrical properties. Pure $CsSnBr_3$ was found by Clark et al. to undergo a semimetal-semiconductor phase transition [7]. The structural and electronic properties of $CsSnBr_3$ have been repeatedly studied experimentally and theoretically [8–17], but there is no data in the literature on the optical properties of orthorhombic $CsSnBr_3$ and iodine-doped $CsSnBr_3$ ($CsSnBr_{3-x}I_x$). In this paper, we report on the optical properties of orthorhombic perovskites based on $CsSnBr_{3-x}I_x$.

2. Materials and Methods

Ab initio quantum chemical calculations within the framework of the density functional theory [6] were implemented in the *Wien2k* package [18] taking into account spin-orbital and spin-polarized effects. DFT is a method based on quantum chemical calculations, originally proposed by Hohenberg [19], Kohn and Sham [20], which has the advantage that it does not depend on any experimental parameters. The modified Becke-Johnson potential (*TB-mBJ*) [21] was used to take into account the exchange-correlation energy (*XC*). The objects of study were orthorhombic structures (Pnma, 62) of nanocrystals of the $CsSnBr_{3-x}I_x$ family. The Muffin sphere radius (RMT) for Cs, Sn, and I was taken to be $2.5a_0$, and for Br, $2.07a_0$, where a_0 is the Bohr radius. The valence wave functions inside the MT sphere were expanded to $l_{\max} = 10$, and the charge density was expanded in a Fourier series up to G_{\max} (boron-1). For the wave function in the interstitial region, the plane wave cutoff value $k_{\max} = 7/RMT$ was chosen. For integration in *k*-space in the Brillouin zone (*BZZ*), a grid of 1000 *k*-points was used. The energy cutoff was chosen to be -6.0 Ry, which determines the separation of the valence and core states. The charge convergence was chosen to be 0.0001e during self-consistency cycles.

2.1. Calculation of Optical Properties

All kinds of solids are characterized by optical characteristics such as absorption, photoconductivity, reflection and transmission spectra, and can be quantified at the microscopic and macroscopic levels. At the microscopic or quantum mechanical level in bulk materials, the complex dielectric function is closely related to the band structure. The calculated optical parameters, such as absorption coefficient and refractive indices, indicate what type of response these materials will exhibit when hit by photons. The real part indicates the stored energy of a material that can be output at zero energy or zero frequency and is considered an intrinsic characteristic of any material. The expression for the complex imaginary permittivity $\varepsilon_2(\omega)$ was obtained by summing over the conduction bands according to [22]:

$$\varepsilon_2^{\alpha\beta}(\omega) = \frac{4\pi^2 e^2}{\Omega} \frac{1}{q^2} \lim_{q \rightarrow 0} \sum_{c,\theta,k} 2\omega_k \delta(\varepsilon_{ck} - \varepsilon_{\theta k} - \omega) \times \langle u_{ck+e_{\alpha}q} | u_{ck} \rangle \langle u_{ck+e_{\alpha}q} | u_{\theta k} \rangle^* \quad (1)$$

According to Equation 1, electrons pass from the occupied to the unoccupied states only within the first Brillouin zone, the wave vectors are fixed *k*. The real and imaginary parts of the analytical permittivity are related by the Kramers-Kronig relation as:

$$\varepsilon_1^{\alpha\beta}(\omega) = 1 + \frac{2}{\pi} P \int_0^{\infty} \lim_{q \rightarrow 0} \frac{\varepsilon_2^{\alpha\beta}(\omega') \omega'}{\omega'^2 - \omega^2 + i\eta} d\omega' \quad (2)$$

Taking into account expression 1 and 2, it is possible to determine the photoconductivity spectrum (σ), energy loss spectrum (*L*), refractive index (*n*), reflection coefficient (*R*), absorption coefficient (α) and extinction coefficient (*k*) as a function of ω in form:

$$R(\omega) = \left| \frac{\sqrt{\varepsilon(\omega)} - 1}{\sqrt{\varepsilon(\omega)} + 1} \right|^2 \quad (3)$$

where $\varepsilon(\omega) = \varepsilon_1(\omega) + i\varepsilon_2(\omega)$.

$$L(\omega) = \frac{\varepsilon_2(\omega)}{\varepsilon_1^2(\omega) + \varepsilon_2^2(\omega)} \quad (4)$$

$$n(\omega) = \left| \frac{\sqrt{\varepsilon_1^2 + \varepsilon_2^2} + \varepsilon_1}{2} \right|^{\frac{1}{2}} \quad (5)$$

$$k(\omega) = \left| \frac{\sqrt{\varepsilon_1^2 + \varepsilon_2^2} - \varepsilon_1}{2} \right|^{\frac{1}{2}} \quad (6)$$

$$\alpha(\omega) = \frac{2\omega k(\omega)}{c} = \frac{\varepsilon_2(\omega)\omega}{n(\omega)c} \quad (7)$$

$$\sigma(\omega) = \sigma_1(\omega) + i\sigma_2(\omega) = -i \frac{\omega}{4\pi} [\varepsilon(\omega) - 1] = \frac{\varepsilon_2(\omega)\omega}{4\pi} + i \frac{1-\varepsilon_1(\omega)\omega}{4\pi} \quad (8)$$

Absorption coefficient reflects the measurement of light absorption ability of ceramics. When light propagates in the medium, the phenomenon of the intensity of light decreases with the propagation distance (penetration depth) is called light absorption. The absorption of light follows the Beer-Lambert law, and its equation is:

$$I = I_0 e^{-KCL} \quad (9)$$

where I is the outgoing Light Intensity; I_0 is the incidental light intensity; K is the molar absorption coefficient, which is dependent on the nature of the absorbent or the wavelength of the incident light and the absorption coefficient is a constant in the Beer-Lambert law; C is the absorbent concentration and L is the absorbent thickness.

Thus, the dielectric function serves as a bridge between the microphysical transition and the electronic structure of a solid, and on the other hand, the main dielectric function can also be used to evaluate other spectral properties of materials.

3. Results and Discussion

The optical properties of the material, according to Maxwell's equations, are based on the characteristic constants of the substance, such as permittivity, magnetic permeability, and electrical conductivity, which are functions of the frequency (ω) of the incident photon [23]. The incident photon interacts with the constituent atoms, and hence the dielectric function $\varepsilon(\omega)$ describes the optical response of the material. Figure 1 (a, b) shows the calculated real $\varepsilon_1(\omega)$ and imaginary $\varepsilon_2(\omega)$ parts of the dielectric functions depending on the photon energy in the range of 0-14 eV from the results of mBJ calculations.

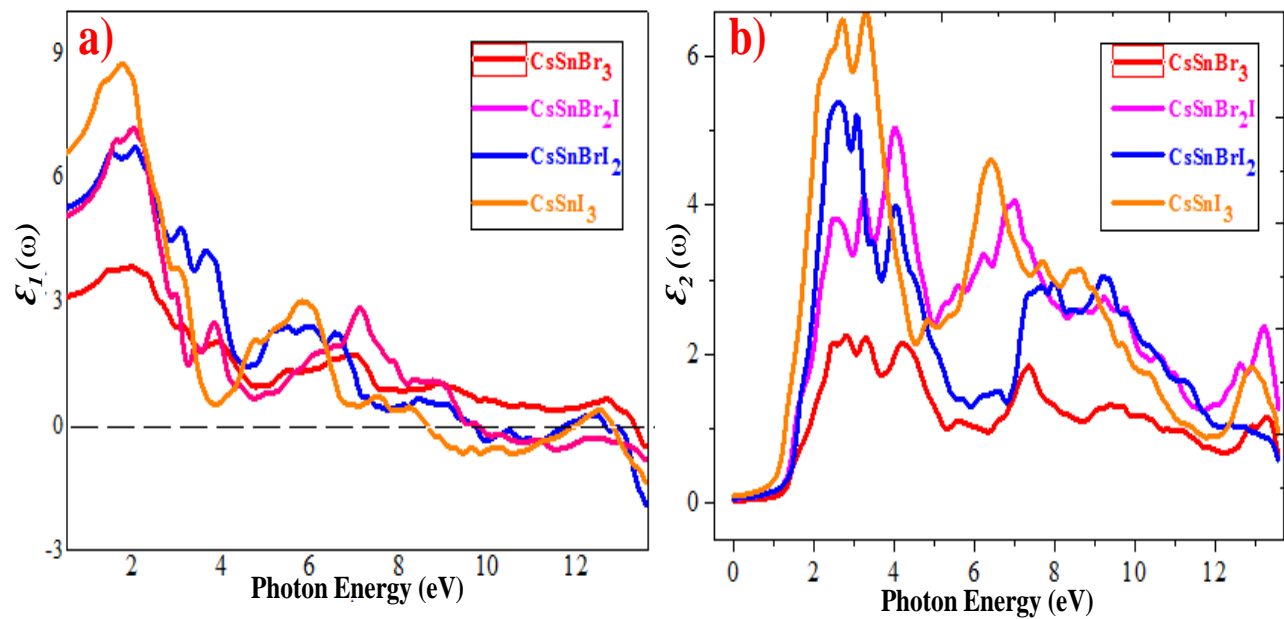


Figure 1. The calculated value of $\varepsilon_1(\omega)$ and $\varepsilon_2(\omega)$ for CsSnBr₃, CsSnI₂Br and CsSnI₃ depending on the photon energy

The real part indicates the stored energy of a material that can be output at zero energy or the zero frequency limit, and is considered an intrinsic characteristic of any material. Figure 1(a) shows that at sufficiently high incident photon energies these materials exhibit metallic behavior. The negative value of ε_1 for these systems indicates their metallic nature. That is, it is possible to investigate and evaluate the metallicity of materials according to a real function. On fig. 1(a) shows that $\varepsilon_1(\omega)$ increases when Br is replaced by I. This is indicated by the inverse relationship between the band gap and $\varepsilon_1(\omega)$.

On the other hand, the imaginary part represents the absorptivity and the behavior of these materials shows the energy gain for photovoltaic devices. The imaginary part of the function $\varepsilon_2(\omega)$ is related to the band structure and describes its behavior upon absorption [24]. An increase in the value of ε_2 and its shift towards long-wavelength radiation in Figure 1(b) indicates that these materials can absorb the maximum amount of energy in a wide range of photon energies and, coincidentally, can retain this energy, and since this ability increases with an increase in the iodine content in the system. In this case, the optical band gap has an inverse relationship between them. Broad spectra of the dielectric function show high absorption in various regions of the energy spectrum. Similar features are found below in the spectra of extinction coefficients (k), absorption coefficients (α).

When light propagates in a medium due to the processes of absorption and scattering, dissipation (weakening) of light occurs - a phenomenon known as light quenching. If scattering plays no role compared to absorption, then the extinction coefficient becomes the same as the absorption coefficient. The measure of light attenuation is the light extinction coefficient (k). On the other hand, the extinction coefficient of materials means how actively a substance absorbs light at a given wavelength. This optical property of the material is also related to the refractive index of the material.

Figures 2 to 4 show the extinction, absorption, and photoconductivity spectra for the $CsSnBr_3$, $CsSnI_2Br_2$, $CsSnI_2Br$, and $CsSnI_3$ systems, respectively, as functions of the photon energy (in the IR range).

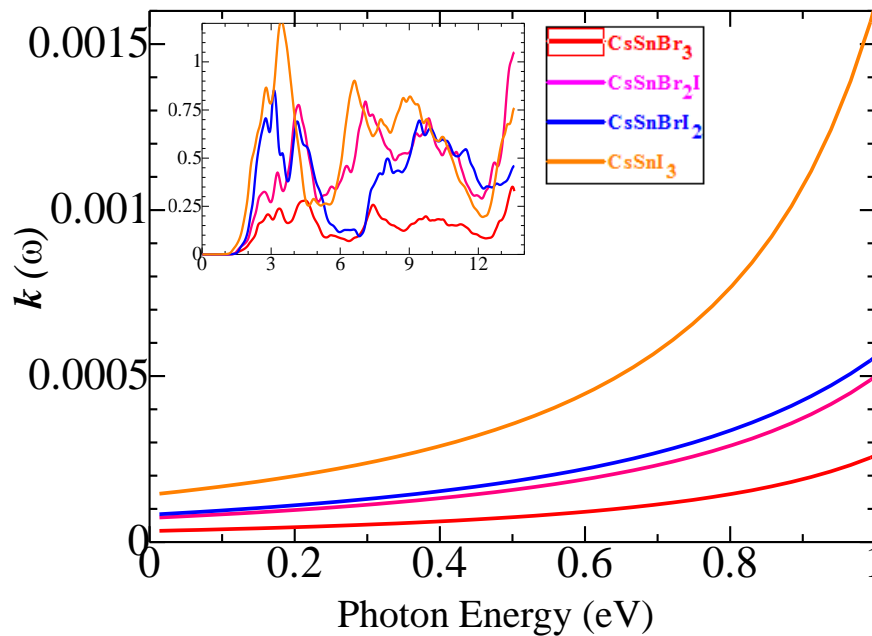


Figure 2. The calculated value of $k(\omega)$ for $CsSnBr_3$, $CsSnI_2Br_2$, $CsSnI_2Br$ and $CsSnI_3$ depending on the photon energy (inset: extinction coefficient ranging from 0 to 14 eV)

A positive value of k indicates that there will be absorption, while it indicates that the light is passing directly through the material [39]. According to Figure 2, the graphs of the extinction coefficients have similar features (critical points) with the imaginary part. The absorption coefficient (α) determines how far in the material the propagation of light can drill through the material before it is absorbed and depends on both the incoming light and the intrinsic properties of the material [25, 26].

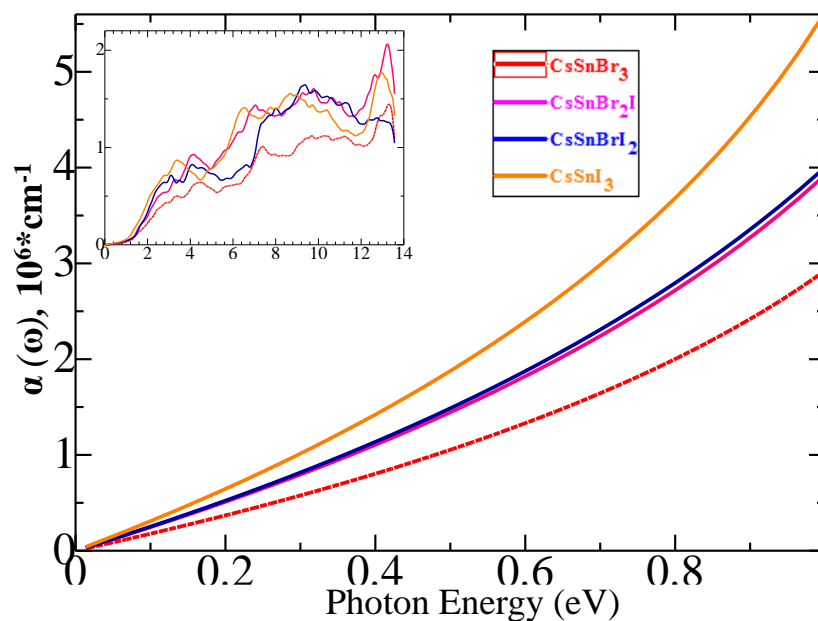


Figure 3. The calculated value of $\alpha(\omega)$ for $CsSnBr_3$, $CsSnI_2Br_2$, $CsSnI_2Br$ and $CsSnI_3$ depending on the photon energy (inset: absorption coefficient ranging from 0 to 14 eV)

According to Figure 3, with a decrease in the content of bromine and an increase in the concentration of iodine, the absorption capacity of the $CsSnBr_{3-x}I_x$ system increases, and therefore $CsSnI_3$ is characterized by maximum absorption in the IR region and will cover the maximum range of the solar spectrum, therefore it is suitable for devices such as solar cells, LEDs and lasers. The maximum extinction and absorption coefficients are in the same range of light, which is consistent with the dispersion theory [27-29].

The optical conductivity spectra $\sigma(\omega)$ shown in Figs. 4 show that the optical conductivity starts at about 0.52, 0.46, 0.23 and 0.18 eV for $CsSnBr_3$, $CsSnBr_2I$, $CsSnBrI_2$ and $CsSnI_3$, respectively. Outside these points, $\sigma(\omega)$ increases and reaches a maximum there, and then decreases again and, finally, dissipates with small variations.

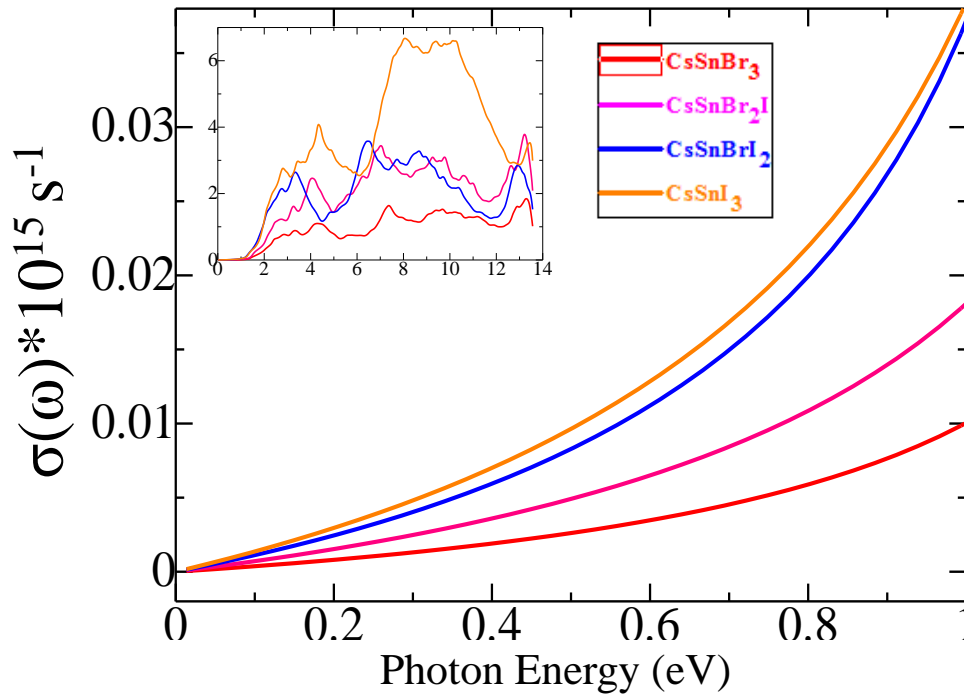


Figure 4. Optical conductivity spectra of the $CsSnBr_{3-x}I_x$ system as a function of energy (insert: $\sigma(\omega)$ in the range from 0 to 14 eV)

The calculated light reflectance spectra $R(\omega)$ for IR radiation are shown in Figure 5 for all investigated materials.

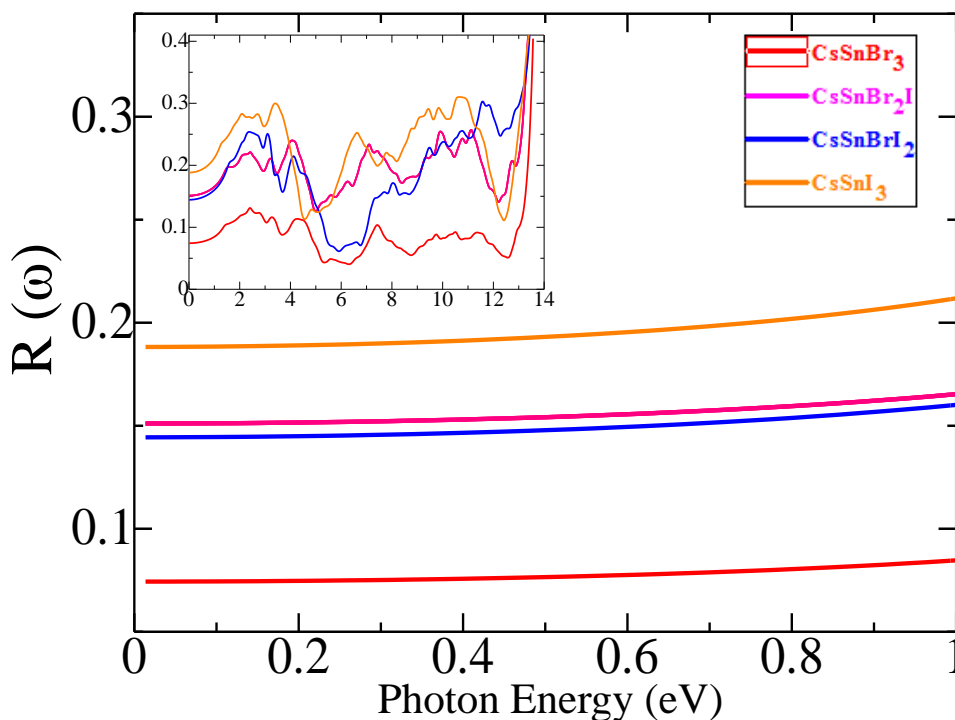


Figure 5. Reflectivity of perovskites of the $CsSnBr_{3-x}I_x$ system depending on the energy (insert: $R(\omega)$ in the range 0 to 14 eV)

According to the results, with an increase in the I content in the system, the reflection coefficient tends to decrease (Figure 5), which is also confirmed by an increase in the absorption coefficients of the materials under study. According to the results of quantum chemical calculations, the maximum reflection occurs when $\epsilon_1(\omega)$ reaches a negative value, i.e. thus, the material exhibits dielectric properties ($\epsilon_1(\omega) > 0$); below zero, the material exhibits metallic properties ($\epsilon_1(\omega) < 0$). The maximum range of $R(\omega)$ increased with increasing metallicity, when $\epsilon_1(\omega)$ became negative.

The electron energy loss functions $L(\omega)$ and the refractive index $n(\omega)$ were calculated using the real and imaginary components of the permittivity from expressions (4 and 5). The electron energy loss function $L(\omega)$ is an important parameter describing the non-adaptable scattering in high accelerated electrons passing through the material, characterizing the plasma frequency (ω_p) associated with it. The peaks of the energy loss function represent the combined character of the plasma resonance as well as the plasma frequency (ω_p), above which the material acts as a dielectric and below which it exhibits a metallic nature. The calculated spectra of the energy loss function for the systems under study are shown in Figure 6.

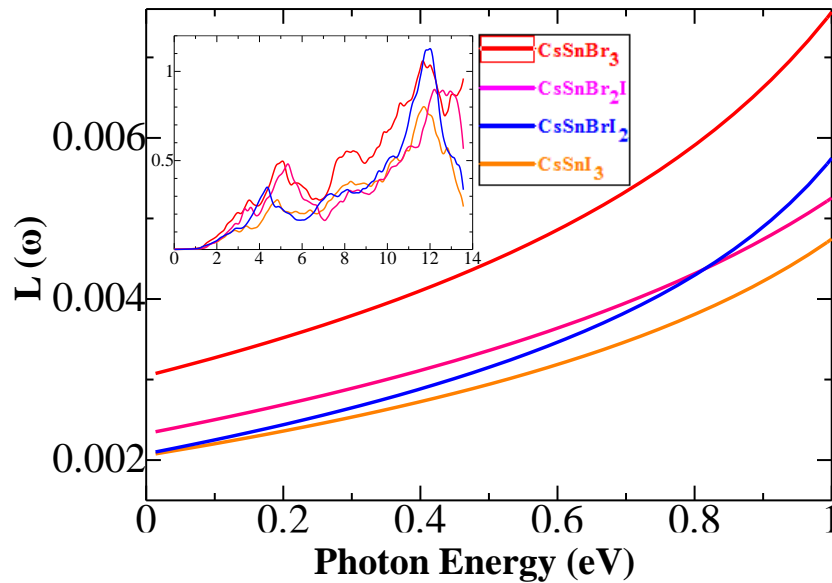


Figure 6. Calculated Energy-Loss Function for CsSnBr_3 , CsSnI_2Br , CsSnI_2Br and CsSnI_3 depending on the energy (insert: $L(\omega)$ in the range from 0 to 14 eV)

According to Figure 6, the energy loss function of CsSnI_3 is the lowest among these perovskites. This is due to the higher electronegativity of I (2.5 on the Pauling scale) compared to Br (2.8 on the Pauling scale). Figure 7 shows the refractive indices $n(\omega)$ as a function of the incident photon energy for the systems under study. All sharp peaks are due to exciton transitions at the band gap allowed in the infrared spectrum.

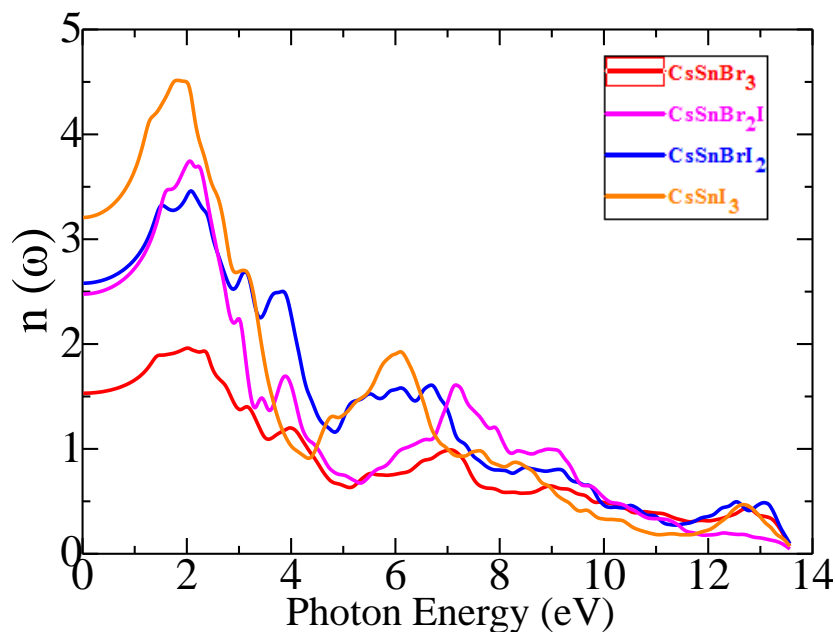


Figure 7. Calculated $n(\omega)$ of perovskites of the $\text{CsSnBr}_{3-x}\text{I}_x$ system depending on the photon energy

From Figure 7 shows that the refractive index $n(\omega)$ of the material increases with increasing iodine concentration in the $CsSnBr_{3-x}I_x$ system. After $n(\omega)$ reached its maximum value, it decreased below unity in some energy ranges. Moreover, considering $n = c/v$, it can be concluded that a refractive index value less than one indicates that the phase velocity of the incident radiation is greater than c , so the incident radiation can penetrate through the depth. Consequently, the material will become transparent to incoming radiation.

The results of calculations of the optical characteristics can be compared with the experimental data, but, as mentioned above, there are no data in the literature on the optical characteristics of the orthorhombic perovskites considered by us. Thus, the results obtained can contribute to the understanding of some features of their optical properties, which are important for the practical application of the studied systems and may be of interest to researchers searching for materials with desired optical characteristics [28-30].

4. Conclusion

The study of the optical properties of the $CsSnBr_{3-x}I_x$ orthorhombic system is very important because of the possibility of its use in LEDs and solar cells. According to the results obtained in this work, it became known that doping with iodine leads to an improvement in the spectral properties of perovskites of the $CsSnBr_{3-x}I_x$ system. It became known that with an increase in the iodine content, the coefficient of extinction, absorbed ability, and photoconductivity of these alloys increase, and in a timely manner, the reflectivity decreases. It was also found that with an increase in the iodine concentration as the transition from $CsSnBr_3$ to $CsSnI_3$ decreases, the electron loss energy decreases. The wide absorption range suggests that these compounds can be used for various optical and optoelectronic devices in all regions of the electromagnetic radiation spectrum.

5. Declarations

5.1. Data Availability Statement

The data presented in this study are available in article.

5.2. Funding

The author received no financial support for the research, authorship, and/or publication of this article.

5.3. Institutional Review Board Statement

Not applicable.

5.4. Declaration of Competing Interest

The author declares that there is no conflict of interests regarding the publication of this manuscript. In addition, the ethical issues, including plagiarism, informed consent, misconduct, data fabrication and/or falsification, double publication and/or submission, and redundancies have been completely observed by the author.

6. References

- [1] Mathur, N., & Littlewood, P. (2003). Mesoscopic texture in manganites. *Physics Today*, 56(1), 25–30. doi:10.1063/1.1554133.
- [2] Moskvina, A. S., Makhnev, A. A., Nomerovannaya, L. V., Loshkareva, N. N., & Balbashov, A. M. (2010). Interplay of p-d and d-d charge transfer transitions in rare-earth perovskite manganites. *Physical Review B - Condensed Matter and Materials Physics*, 82(3), 35106. doi:10.1103/PhysRevB.82.035106.
- [3] Weeks, C., & Franz, M. (2010). Topological insulators on the Lieb and perovskite lattices. *Physical Review B - Condensed Matter and Materials Physics*, 82(8), 85310. doi:10.1103/PhysRevB.82.085310.
- [4] Murtaza, G., Ahmad, I., Amin, B., Afaq, A., Maqbool, M., Maqssod, J., Khan, I., & Zahid, M. (2011). Investigation of structural and optoelectronic properties of BaThO 3. *Optical Materials*, 33(3), 553–557. doi:10.1016/j.optmat.2010.10.052.
- [5] Kagan, C. R., Mitzi, D. B., & Dimitrakopoulos, C. D. (1999). Organic-inorganic hybrid materials as semiconducting channels in thin-film field-effect transistors. *Science*, 286(5441), 945–947. doi:10.1126/science.286.5441.945.
- [6] Green, M., Dunlop, E., Hohl-Ebinger, J., Yoshita, M., Kopidakis, N., & Hao, X. (2021). Solar cell efficiency tables (version 57). *Progress in Photovoltaics: Research and Applications*, 29(1), 3–15. doi:10.1002/pip.3371.
- [7] Clark, S. J., Flint, C. D., & Donaldson, J. D. (1981). Luminescence and electrical conductivity of CsSnBr₃, and related phases. *Journal of Physics and Chemistry of Solids*, 42(3), 133–135. doi:10.1016/0022-3697(81)90072-X.
- [8] Parry, D. E., Tricker, M. J., & Donaldson, J. D. (1979). The electronic structure of CsSnBr₃ and related trihalides; Studies using XPS and band theory. *Journal of Solid State Chemistry*, 28(3), 401–408. doi:10.1016/0022-4596(79)90092-6.
- [9] Shum, K., Chen, Z., Qureshi, J., Yu, C., Wang, J. J., Pfenninger, W., Vockic, N., Midgley, J., & Kenney, J. T. (2010). Synthesis and characterization of CsSnI₃ thin films. *Applied Physics Letters*, 96(22), 221903. doi:10.1063/1.3442511.

- [10] Bose, S. K., Satpathy, S., & Jepsen, O. (1993). Semiconducting CsSnBr₃. *Physical Review B*, 47(8), 4276–4280. doi:10.1103/PhysRevB.47.4276.
- [11] Lefebvre, I., Lippens, P. E., Lannoo, M., & Allan, G. (1990). Band structure of CsSnBr₃. *Physical Review B*, 42(14), 9174–9177. doi:10.1103/PhysRevB.42.9174.
- [12] Davlatshoevich, N. D., Ashur, K. M., Saidali, B. A., Kholmirtotagoykulovich, K., Lyubchik, A., & Ibrahim, M. (2022). Investigation of structural and optoelectronic properties of N-doped hexagonal phases of TiO₂ (TiO₂-xNx) nanoparticles with DFT realization: Optimization of the band gap and optical properties for visible-light absorption and photovoltaic applications. *Biointerface Research in Applied Chemistry*, 12(3), 3836–3848. doi:10.33263/BRIAC123.38363848.
- [13] Doroshkevich, A. S., Nabiev, A. A., Shylo, A. V., Pawlukoć, A., Doroshkevich, V. S., Glazunova, V. A., ... Bodnarchuk, V. I. (2019). Frequency modulation of the Raman spectrum at the interface DNA - ZrO₂ nanoparticles. *Egyptian Journal of Chemistry*, 62(1), 13–15. doi:10.21608/ejchem.2019.12898.1806.
- [14] Nematov, D. D., Burhonzoda, A. S., Khusenov, M. A., Kholmurodov, K. T., & Yamamoto, T. (2021). First Principles Analysis of Crystal Structure, Electronic and Optical Properties of CsSnI₃-xBr_x Perovskite for Photoelectric Applications. *Journal of Surface Investigation*, 15(3), 532–536. doi:10.1134/S1027451021030149.
- [15] Nematov, D. D., Burhonzoda, A. S., Khusenov, M. A., Kholmurodov, K. T., Elhaes, H., & Ibrahim, M. A. (2019). The quantum-chemistry calculations of electronic structure of boron nitride nanocrystals with density functional theory realization. *Egyptian Journal of Chemistry*, 62, 21–27. doi:10.21608/EJCHEM.2019.12879.1805.
- [16] Nematov, D. D., Kholmurodov, K. T., Yuldasheva, D. A., Rakhmonov, K. R., & Khojakhonov, I. T. (2022). Ab-initio Study of Structural and Electronic Properties of Perovskite Nanocrystals of the CsSn[Br_{1-x}I_x]₃ Family. *HighTech and Innovation Journal*, 3(2), 140–150. doi:10.28991/hij-2022-03-02-03.
- [17] Verma, A. S., Kumar, A., & Bhardwaj, S. R. (2008). Correlation between ionic charge and the lattice constant of cubic perovskite solids. *Physica Status Solidi (B) Basic Research*, 245(8), 1520–1526. doi:10.1002/pssb.200844072.
- [18] Blaha, P., Schwarz, K., Tran, F., Laskowski, R., Madsen, G. K. H., & Marks, L. D. (2020). WIEN2k: An APW+lo program for calculating the properties of solids. *Journal of Chemical Physics*, 152(7), 74101. doi:10.1063/1.5143061.
- [19] Hohenberg, P., & Kohn, W. (1964). Inhomogeneous electron gas. *Physical Review*, 136(3B), 864–871. doi:10.1103/PhysRev.136.B864.
- [20] Kohn, W., & Sham, L. J. (1965). Self-consistent equations including exchange and correlation effects. *Physical Review*, 140(4A), 1133–1138. doi:10.1103/PhysRev.140.A1133.
- [21] Koller, D., Tran, F., & Blaha, P. (2011). Merits and limits of the modified Becke-Johnson exchange potential. *Physical Review B - Condensed Matter and Materials Physics*, 83(19). doi:10.1103/PhysRevB.83.195134.
- [22] Gajdoš, M., Hummer, K., Kresse, G., Furthmüller, J., & Bechstedt, F. (2006). Linear optical properties in the projector-augmented wave methodology. *Physical Review B - Condensed Matter and Materials Physics*, 73(4), 45112. doi:10.1103/PhysRevB.73.045112.
- [23] Afsari, M., Boochani, A., & Hantezadeh, M. (2016). Electronic, optical and elastic properties of cubic perovskite CsPbI₃: Using first principles study. *Optik*, 127(23), 11433–11443. doi:10.1016/j.ijleo.2016.09.013.
- [24] Ghaithan, H. M., Alahmed, Z. A., Lyras, A., Qaid, S. M. H., & Aldwayyan, A. S. (2020). Computational Investigation of the Folded and Unfolded Band Structure and Structural and Optical Properties of CsPb(I_{1-x}Br_x)₃ Perovskites. *Crystals*, 10(5), 342. doi:10.3390/cryst10050342.
- [25] Zafar, M., Kashif Masood, M., Rizwan, M., Zia, A., Ahmad, S., Akram, A., Bao, C. C., & Shakil, M. (2019). Theoretical study of structural, electronic, optical and elastic properties of Al_xGa_{1-x}P. *Optik*, 182, 1176–1185. doi:10.1016/j.ijleo.2018.12.165.
- [26] Zafar, M., Shakil, M., Ahmed, S., Raza-ur-Rehman Hashmi, M., Choudhary, M. A., & Naeem-ur-Rehman. (2017). Ab initio study of structural, electronic and elastic properties of CdSe_{1-x}S_x semiconductor. *Solar Energy*, 158, 63–70. doi:10.1016/j.solener.2017.09.034.
- [27] Feinberg, G., Sucher, J., & Au, C. K. (1989). The dispersion theory of dispersion forces. *Physics Reports*, 180(2), 83–157. doi:10.1016/0370-1573(89)90111-7.
- [28] Lin, J., Yu, M., Lin, C., & Liu, X. (2007). Multifunctional Oxide Optical Materials via the Versatile Pechini-Type Sol-Gel Process: Synthesis and Characteristics. *The Journal of Physical Chemistry C*, 111(16), 5835–5845. doi:10.1021/jp070062c.
- [29] Xin, H., Holewinski, A., Schweitzer, N., Nikolla, E., & Lincic, S. (2012). Electronic Structure Engineering in Heterogeneous Catalysis: Identifying Novel Alloy Catalysts Based on Rapid Screening for Materials with Desired Electronic Properties. *Topics in Catalysis*, 55(5-6), 376–390. doi:10.1007/s11244-012-9794-2.